Research Article | Vol. 10, No. 8 | 1 Aug 2019 | BIOMEDICAL OPTICS EXPRESS 4305
Biomedical Optics EXPRESS

Diffuse optical tomography of the breast: a potential modifiable biomarker of breast cancer risk with neoadjuvant chemotherapy

Mirella L. Altoe,[1] Alessandro Marone,[1] Hyun K. Kim,[2] Kevin Kalinsky,[3] Dawn L. Hershman,[3] Andreas H. Hielscher[1,2,4] and Richard S. Ha[2,*]

[1]*Department of Biomedical Engineering, Columbia University, 500 W 120th St, Mudd Bldg, ET351, New York, NY 10027, USA*
[2]*Department of Radiology, Columbia University Irving Medical Center, 622 W 168th Street, New York, NY 10032, USA*
[3]*Department of Medicine, Division of Hematology/Oncology, Columbia University Irving Medical Center, 1130 St. Nicholas Avenue, New York, NY 10032, USA*
[4]*Department of Electrical Engineering, Columbia University, 500 W 120th St, Mudd Bldg, MC 8904, New York, NY 10027, USA*
**rh2616@cumc.columbia.edu*

Abstract: The purpose of this study is to evaluate whether a diffuse optical tomography breast imaging system (DOTBIS) can provide a comparable optical-based image index of mammographic breast density, an established biomarker of breast cancer risk. Oxyhemoglobin concentration (ctO_2Hb) measured by DOTBIS was collected from 40 patients with stage II-III breast cancer. The tumor-free contralateral breast was used for this evaluation. We observed a moderate positive correlation between the patient's mammogram density classification and ctO_2Hb, $r_s = 0.486$ ($p = 0.001$). In addition, significant reduction in ctO_2Hb levels were noted during neoadjuvant chemotherapy treatment ($p = 0.017$). This observation indicates that ctO_2Hb levels measured by DOTBIS could be a novel modifiable imaging biomarker of breast cancer risk and warrants further investigation.

1. Introduction

According to the American Cancer Society, breast cancer accounts for one third of all new cancer diagnoses in women. In the United States, one in eight women will develop breast cancer during their lifetimes and about 40,000 women are expected to die in 2019 from breast cancer [1]. Therefore, providing risk prediction tools are of great clinical need to better address personalized screening of high-risk women, and even for recommendation of chemoprevention treatments based on a patient's risk of developing breast cancer.

One of the most well established imaging biomarker of breast cancer risk is mammographic density [2–4]. Women with mammographically dense breasts have a higher risk of breast cancer than women with less dense breasts [5,6].The mammographic breast density equivalent in breast magnetic resonance imaging (MRI) is fibroglandular tissue (FGT) and has also been shown to correlated with breast cancer risk [7–9].

However, both X-ray mammography and MRI have several drawbacks. Mammography generates 2-dimensional (2D) images and the amount of breast density can vary due to changes in positioning [10]. Given this limitation, mammogram has limited ability to quantify longitudinal density variations accurately. In addition, its use of ionizing radiation restricts a long scale screening. Breast MRI overcomes the limitations of mammogram providing 3-dimensional (3D) evaluation of the fibroglandular tissue. However, high cost, intravenous injection, and long duration of exam limits its routine use.

#362299 https://doi.org/10.1364/BOE.10.004305
Journal © 2019 Received 13 Mar 2019; revised 19 Jun 2019; accepted 21 Jun 2019; published 1 Aug 2019

Biomedical Optics EXPRESS

In recent years, several groups [11–14] have shown evidence that optical based imaging modalities may play an important role in assessing breast tissue composition by measuring optical property contrast from endogenous chromophores. The advantages of optical techniques are the use of non-ionizing radiation, ease of use, and relatively low cost. We developed a diffuse optical tomography breast imaging system (DOTBIS) which does not require the use of contrast agents or compression, and enables imaging of the whole volume for both breasts simultaneously using low intensity near infrared light capable to measure tissue concentration of total hemoglobin (ctTHb), oxy-hemoglobin (ctO_2Hb), deoxy-hemoglobin (ctHHb), oxygen saturation (StO_2) and water percentage.

We hypothesize that diffuse optical tomography imaging provides quantitative measurements of tissue functional components, such as ctO_2Hb, which is directly related to tissue metabolism and vascular characteristics, and could be correlated to mammographic breast density, a known imaging biomarker of breast cancer risk [15]. In addition, we evaluate whether DOTBIS-measured oxyhemoglobin concentration is modifiable after neoadjuvant chemotherapy (NAC).

2. Materials and methods

This retrospective cohort study analyzed 40 patients with stage II-III breast cancer in a Columbia University Institutional Review Board (IRB) clinical protocol. The patient inclusion criteria for this subset were defined by availability of DOTBIS measurements at baseline, after two cycles of taxol drug infusion or at the end of NAC, and available mammographic breast density assessment before starting NAC. Each patient received a taxane-based regimen. Out of 40 patients, 32 subjects (80%) received 12 cycles of weekly paclitaxel followed by 4 cycles of doxorubicin and cyclophosphamide given every 2 weeks with growth-factor support (T x 12/AC x 4). Two patients received the same treatment but with an addition of carboplatin to paclitaxel (T/C x 12/AC x 4). Three patients received six cycles of docetaxel, carboplatin, and trastuzumab plus pertuzumab (TCHP). Lastly, another three patients received six cycles cytoxan plus taxotere (T/C x 6). Subject demographics according to DOTBIS imaging availability at baseline, after two cycles of chemotherapy, and at the end of therapy prior to surgery, are shown in Table 1.

Table 1. Subject demographics according to NAC regimen and its DOTBIS imaging availability.

NAC Regimen	Age[a]	BMI	No. of patients		
			Baseline	Before 3rd cycle	Pre-surgery
T x 12/AC x 4	48.00 ± 10.85	29.65 ± 6.40	32	30	19
T/C x 12/AC x 4	35.00 ± 2.00	30.11 ± 2.71	2	0	2
T/C x 6	67.33 ± 2.49	28.61 ± 3.91	3	2	0
TCHP	51.67 ± 3.86	27.35 ± 5.54	3	3	3

[a]Average and standard deviation (range) of continuous variable. Abbreviations and Acronyms: NAC, neoadjuvant chemotherapy; T x 12/AC x 4, 12 cycles of weekly paclitaxel followed by 4 cycles of doxorubicin and cyclophosphamide given every 2 weeks with growth-factor support; T/C x 12/AC x 4, 12 cycles of weekly paclitaxel followed by 4 cycles of doxorubicin and cyclophosphamide given every 2 weeks with growth-factor support with an addition of carboplatin to paclitaxel T/C x 6, six cycles cytoxan plus taxotere; TCHP, six cycles of docetaxel, carboplatin, and trastuzumab plus pertuzumab; BMI, Body Mass Index.

2.1 Mammographic breast density measurement

Mammograms at our institution were performed on dedicated mammography units (Senographe Essential, GE Healthcare). The views obtained consisted of the standard mediolateral oblique and craniocaudal views. Additional views were obtained if clinically indicated or requested by the reading radiologist. A breast fellowship trained radiologist with 7 years of experience, blinded to the DOT measures, classified mammographic breast density (BD) in accordance with BI-RADS categories: BD I = almost all fatty tissue, BD II =

Biomedical Optics EXPRESS

scattered areas of dense glandular and fibrous tissue, BD III = heterogeneously dense and BD IV = extremely dense.

2.2 DOTBIS measurement

By sampling the entire breast volume, the three-dimensional (3D) maps of ctTHb, ctO_2Hb, ctHHb, StO_2% and water percentage for the contralateral normal breast were performed using a continuous-wave DOTBIS described in details in [16]. The patient interface consists of two sets of four rings that can be adjusted to provide different setting depending on patient breast cup, Fig. 1.

Fig. 1. Left: photograph of the custom-built diffuse optical tomographic breast imaging system (DOTBIS). Right: patient placed in the probe for imaging. The patient interface consists of two sets of four rings that can be adjusted to provide customized setting for different breast cup sizes.

Total measurement time varied between 6 to 8 minutes in addition to 5 minutes required to set up the machine and adjust patient interface. In summary, the system uses four laser diode sources (765, 808, 827 and 905 nm) that illuminate both breasts and then acquires data from 32 sources and 64 detectors per breast. The spatial distribution of chromophore concentrations is obtained by a PDE-constrained multispectral imaging method [17] which uses the diffusion approximation to the equation of radiative transfer to describe the light propagation in such scattering-dominated media as the breast tissue. Tomographic distributions of each chromophore were averaged over the breast volume for feature extraction. For visualization, maximum intensities projections (MIP) were obtained from the 3D image maps. MIP projects the acquired data volume into a view plane, which can be obtained by finding the voxels with maximum intensity along a chosen axis. For post-processing analyses, nipple region was excluded so any variability from this highly vascularized region in inter and intra-patient analyses could be diminished. For visualization purposes only, the nipple was replaced by the lowest voxel intensity value.

2.3 Statistical analyses

Statistical analyses were computed using the statistical software program SPSS version 16.0 (SPSS, Chicago, IL, USA). A Spearman's rank-order correlation was run to assess the relationship between mammographic breast density and ctTHb, ctO_2Hb, ctHHb, StO_2% and water percentage measured at baseline. Next, a Kruskal-Wallis test was conducted to determine if there were differences in baseline ctTHb, ctO_2Hb, ctHHb, StO_2% and water percentage levels between the breast density groups. A paired-samples t-test was used to determine whether there was a statistically significant mean difference between DOTBIS-measured parameters at baseline compared to after two cycles of NAC, and at the end of therapy, and between responder and non-responder tumors. Significance was assumed at a confidential interval of 95% ($p = 0.05$).

Biomedical Optics EXPRESS

3. Results

We assessed BD from mammogram available before starting NAC. BD I category was present in 2% of the patients (n = 1), BD II in 43% (17/40), BD III in 53% (21/40) and BD IV in 2% (n = 1). Figure 2 displays the mammogram and DOTBIS reconstructions at baseline for four subjects with different BI-RADS classification.

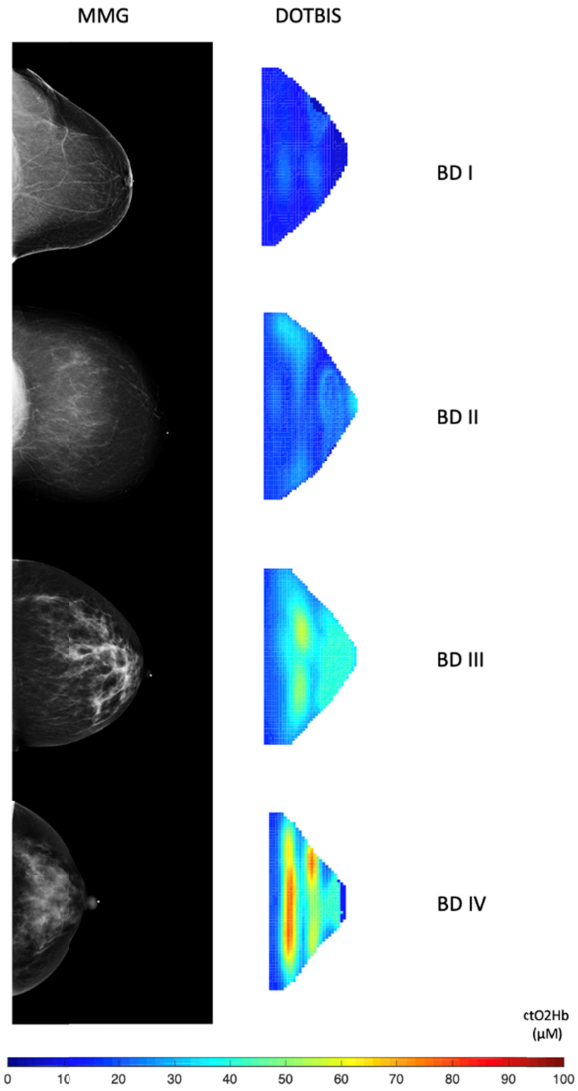

Fig. 2. Corresponding mammogram (MMG) and DOTBIS image. MIP images (axial orientation) were acquired at baseline in the contralateral normal breast of 42-year-old women (BD I), 40-year-old women (BD II), a 36-year-old women (BD III) and a 46-year-old women (BD IV). Nipples were excluded.

Spearman's rank-order correlation was run to assess the relationship between DOTBIS-measured water and hemoglobin concentrations at baseline, and mammographic breast density. As shown by Table 2, there was a moderate positive correlation between baseline ctO_2Hb and BD, $r_s = 0.486$, $p = 0.001$. Baseline ctTHb, $r_s = 0.426$, $p = 0.006$, and water percentage level, $r_s = 0.322$, $p = 0.042$, were also statistically significant correlated with breast

Biomedical Optics EXPRESS

density. After running multivariate correlative analysis, ctO_2Hb combined to water percentage level was also associated with breast density categories, $r_s = 0.497$, $p = 0.001$.

Table 2. Baseline ctTHb, ctO_2Hb, ctHHb, StO_2 and water percentage (mean ± standard deviation) for all the different BI-RADS classification and their specific Spearman's correlation coefficient with breast density. Bold values indicate statistical significance at $p < 0.05$ level.

DOTBIS features	BD I (n = 1)	BD II (n = 17)	BD III (n = 21)	BD IV (n = 1)	Spearman's correlation coefficient	p-value
ctTHb (μM)	20.66	26.91 ± 9.58	35.76 ± 12.64	48.67	**.426**	**.006**
ctO_2Hb (μM)	12.63	15.41 ± 5.84	21.88 ± 8.10	29.04	**.486**	**.001**
ctHHb (μM)	8.00	11.50 ± 4.57	13.87 ± 6.02	19.63	0.277	0.084
Water (%)	52.74	45.72 ± 9.15	51.14 ± 5.38	55.10	**.327**	**.040**
StO_2 (%)	61.20	58.47 ± 6.01	61.60 ± 6.03	60.97	0.205	0.205

A Kruskal-Wallis H test was conducted to determine if there were differences in baseline of ctTHb, ctO_2Hb, ctHHb, StO_2 and water percentage levels between the breast density groups, Table 3. Median ctO_2Hb levels were the only parameter statistically significant different between BD groups, $\chi 2(2) = 9.374$, $p = 0.025$, and increased from BD I (12.00 μM), to BD II (14.65 μM), to BD III (24.95 μM) to BD IV (35.00 μM), Fig. 3 (mean ± standard deviation are shown in Table 3). Subsequently, pairwise comparisons were performed using Dunn's procedure. A Bonferroni correction for multiple comparisons was made with statistical significance accepted at the $p < 0.008$ level. This post hoc analysis revealed statistically significant differences in ctO_2Hb levels between BD II and BD III, $p = 0.007$. No significant results were available for the comparison with BD I or BD IV which is likely due to the small sample size for both groups (n = 1 for BD IV and BD I).

Table 3. Baseline ctTHb, ctO_2Hb, ctHHb, StO_2 and water percentage (median) for all the different BI-RADS classification. Bold values indicate statistical significance at $p < 0.05$ level after running a Kruskal-Wallis H test to determine if there were differences in baseline DOTBIS-measured parameters between the four breast density groups.

DOTBIS features	BD I (n = 1)	BD II (n = 17)	BD III (n = 21)	BD IV (n = 1)	p-value
ctTHb (μM)	10.00	15.76	24.05	37.00	0.57
ctO_2Hb (μM)	12.00	14.65	24.95	35.00	**.025**
ctHHb (μM)	8.00	18.12	22.24	37.00	0.230
Water (%)	24.00	15.76	23.71	30.00	0.163
StO_2 (%)	23.00	17.35	22.86	22.00	0.542

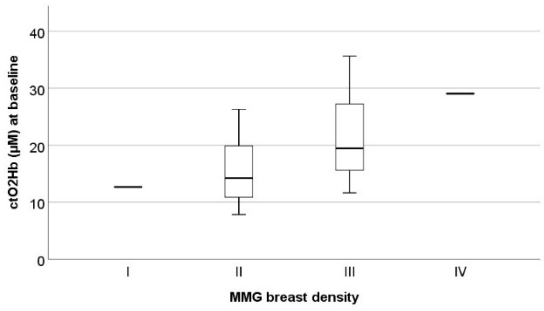

Fig. 3. Simple box plot of ctO_2Hb (μM) in the contralateral breast at baseline for different mammogram (MMG) breast density groups (I = almost all fatty tissue, II = scattered areas of dense glandular and fibrous tissue, III = heterogeneously dense and IV = extremely dense). Group I and IV had only one patient each. There was a moderate positive correlation between ctO_2Hb at baseline and breast density ($r_s = 0.486$, $p = 0.001$).

Biomedical Optics EXPRESS

Thirty-five patients were also imaged after their second cycle of NAC. The first two NAC cycles elicited an overall decrease in ctO_2Hb levels in 60% (21/35) of the patients, whereas 40% (14/35) participants had their ctO_2Hb levels slightly increased. Table 4 summarizes the mean values for of ctTHb, ctO_2Hb, ctHHb, StO_2 and water percentage at three different time points: baseline, after two cycles of taxol drug infusion and at the end of NAC. In Fig. 4, using a grouped scatter plot and drawing a line of equality, we can interpret the overall ctO_2Hb reduction after two NAC cycles (left), and after NAC completion (right). The patients lying on the line correspond to contralateral breast tissue which experience no change to ctO_2Hb levels. Those above the line were higher after two NAC cycles than before at baseline, i.e. display an increase in ctO_2Hb, and those below the line have experienced a reduction in ctO_2Hb. One can notice that majority of the patients are below the line. A paired-samples t-test was used to determined that there was a statistically significant mean decrease in ctO_2Hb levels of 2.39 (95% CI, 0.67 to 4.11) μM after two NAC cycles completion (17.04 ± 7.22 μM) in comparison with ctO_2Hb levels at baseline (19.43 ± 8.17 μM), $p = 0.008$. The mean reduction of 3.22 (95% CI, 0.55 to 6.85) μM after NAC completion (n = 24) was also statistically significant, $p = 0.024$. Statically significant mean reduction was also observed for ctTHb after 2 weeks of therapy, $p = 0.011$, as shown in Table 4. Data are mean ± standard deviation. For better visualization of the longitudinal hemoglobin reduction trend across NAC, Fig. 5 display the mean values of ctO_2Hb levels for eighteen patients imaged at all the 3 time points.

Table 4. ctTHb, ctO_2Hb, ctHHb, StO_2 and water percentage (mean ± standard deviation) at three different time points: baseline, after 2 cycles of taxol and at the end of NAC. Bold values indicate statistical significance at $p < 0.05$ level after running a paired-samples t-test to determine if there was a statistically significant mean decrease in the DOTBIS-measured features after 2 cycles of NAC and at the end of therapy.

DOTBIS features	Baseline (n = 40)	After 2 weeks of NAC (n = 35)	at the end of NAC (n = 20)	Mean difference after 2 week of NAC (n = 35)	Mean difference at the end of NAC (n = 20)
ctTHb (μM)	31.94 ± 12.20	28.73 ± 11.20	30.82 ± 11.10	**3.88 ± 1.44 (p = 0.011)**	5.13 ± 2.52 (p = 0.056)
ctO_2Hb (μM)	19.08 ± 7.83	17.04 ± 7.22	17.33 ± 6.53	**2.39 ± 0.84 (p = 0.008)**	**3.22 ± 1.5 (p = 0.024)**
ctHHb (μM)	12.86 ± 5.50	11.71 ± 4.92	13.48 ± 5.29	1.47 ± 0.74 (p = 0.056)	1.43 ± 1.28 (p = 0.276)
Water (%)	48.98 ± 7.60	46.99 ± 11.36	48.83 ± 7.12	2.31 ± 1.53 (p = 0.141)	0.3 ± 0.1 (p = 0.765)
StO_2 (%)	60.24 ± 5.99	58.51 ± 10.82	57.68 ± 5.16	1.76 ± 1.54 (p = 0.262)	1.71 ± 1.12 (p = 0.143)

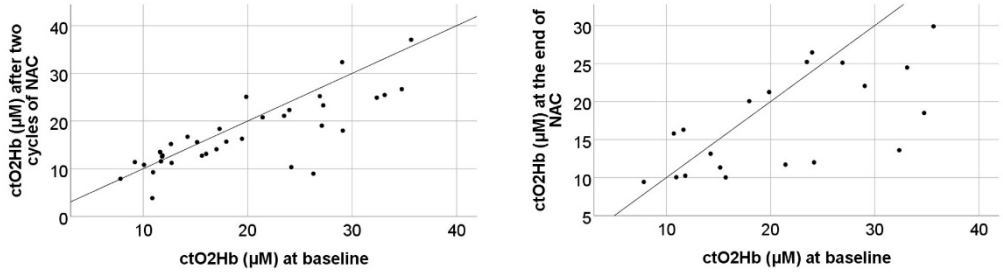

Fig. 4. Left: Grouped scatter plot for reduction comparison between ctO_2Hb (μM) at baseline versus ctO_2Hb before third NAC cycle (n = 35). Right: Grouped scatter plot for reduction comparison between ctO_2Hb (μM) at baseline versus after NAC completion (n = 24).

Biomedical Optics EXPRESS

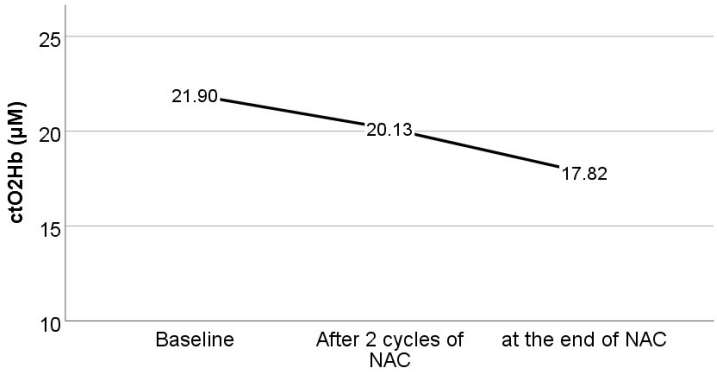

Fig. 5. Mean values of ctO_2Hb levels across NAC therapy for the patients imaged at all the 3 time points (n = 18).

Out of these 35 subjects who were imaged at time point baseline and two weeks after NAC, 26 had their residual cancer burden (RCB) scores available after NAC. To explore any correlation between changes in DOTBIS-measured parameters after 2 cycles of chemotherapy and tumor response, we run an independent-samples t-test to evaluate whether there was a difference between responders (RCB0) and non-responders (RCBI, II and III). The reduction levels of ctO_2Hb, ctTHb, ctHHb, StO_2 and water percentage were not statistically different between responders and non-responder tumors. For instance, the results show a mean difference of 1.80 ± 2.44 μM in ctO_2Hb levels after 2 weeks of NAC between responders and non-responders, but it is not statistically significant (p = 0.468).

The association with age was analyzed by considering ctO_2Hb levels at baseline for all the 40 patients. A linear regression fitting indicates a moderate negative correlation between baseline ctO_2Hb and age (r = –0.439, p = 0.005). From the coefficient of determination, r^2 = 0.20, we can determine that 20% of the variability in baseline ctO_2Hb is explained by patient age at enrollment, Fig. 6.

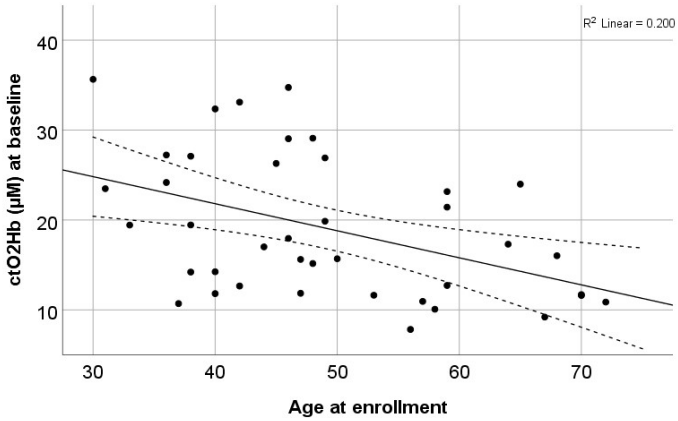

Fig. 6. A linear regression fitting indicates a moderate negative correlation between baseline ctO_2Hb and age (r = –0.439, p = 0.005). The scatterplot shows line of the best fit and its confidence and prediction interval.

Biomedical Optics EXPRESS

4. Discussion

In our study, there was a moderate positive correlation between ctO_2Hb and patient's mammographic density classification. Baseline ctTHb and water percentage level were also statistically significant correlated with breast density. High levels of ctO_2Hb can be associated with the increased rate of metabolism in dense breasts due to the greater volume fraction of fibroglandular tissue compared to almost entirely fat, and the increased vascular demand required by dense tissues. Additionally, the moderate correlation with water can be related to higher water fraction in fibroglandular tissue compared to adipose tissue [18]. This observation indicates that the ctO_2Hb levels measured by DOTBIS may be a novel biomarker of breast cancer risk.

Previous publications, summarized by Grosenick *et al* in their review of optical breast imaging and spectroscopy [19], have shown the feasibility of optically derived data to quantify breast density. Simick *et al.* categorized density measurements into two groups and presented a PCA model that predicts lower from high-density tissues with 80% of accuracy [20]. In addition, Blackmore *et al.* correlated breast tissue optical content (water, lipid and StO_2) with percent density in pre- and post-menopausal women [21]. In a simulation study, Ruiz *et al.* found that estimated percent breast density predicted from lipid and water maps was highly correlated to the true values from MRI [22]. Moreover, Fang *et al.* found linear correlation between ctTHb and the fibroglandular volume fraction derived from the 3D digital breast tomosynthesis imaging scans [23]. However, none of these references specifically correlates the optical data with the four breast density groups from BI-RADS classification, or investigates the changes across NAC treatment.

Similar to our study, O'Sullivan *et al.* demonstrated a moderate correlation between ctTHb level and FGT assessed by MR imaging, $r = 0.597$, $p = 0.040$ [14]. However, they did not find significant correlation with BIRADS classification of mammographic breast density, possibly due to lower number of patients in their study ($n = 12$). They observed significant difference between mean hemoglobin levels in BD II and BD IV, and water percentage levels in BD III and BD IV. With the larger sample size in our study ($n = 40$), we were able to detect a significant difference in mean ctO_2Hb levels between BD II and BD III, a result not observed previously. In addition, unlike our study, the diffuse optical spectroscopy imaging system used in their study did not sample the entire breast volume, and it is unclear if the nipple region was excluded, which can impact accurate assessment due to varied levels of ctO_2Hb involving the nipple. Taroni *et al.* also published a work showing direct correlation between mammographic breast density BI-RADS classification and water, lipid and collagen content. However, for a sample size of 49 patients, the correlation between breast density and ctTHb or StO_2 were not statistically significant [24]. It is important to highlight that the lacking of strong correlation with BI-RADS classification could also be justified by the qualitative measurement approach associated to this type of breast density assessment. High variability between radiologists are expected [25] and quantitative measurements of breast density could reveal stronger association with the optical features.

Because optical imaging provides quantitative metrics capable to measure and track changes in breast tissue composition, we reconstructed the 3D full volume of ctTHb, ctO_2Hb, ctHHb, StO_2 and water percentage maps of 40 patients undergoing NAC treatment to determine whether this metric is modifiable. Our results indicate significant reduction in ctO_2Hb levels after NAC completion. Several studies have reported a consistent reduction of breast density after NAC [26–29]. By using MRI or mammographic imaging, all these groups were able to detect change in percent breast density across NAC. For example, Chen *et al*., using 3D MR imaging, demonstrated that patients who underwent AC and taxane had a mean percentage reduction of 12.7% at the end of NAC [27]. Besides, Sandberg *et al.* and Knight *et al*. took a step further and showed that women who experienced a decrease of at least 10% in breast density after chemotherapy or tamoxifen, had decreased their risk in half of contralateral breast cancer. According to the literature, chemotherapy, including taxane based

Biomedical Optics EXPRESS

regimens, has been linked with amenorrhea and ovarian function suppression. The rapid reduction in estrogen from chemotherapy induced menopause contributes to secondary change in breast tissue composition, and consequently, an impact in mammographic breast density [30,31]. In similar fashion, our results showed that ctO_2Hb measured by DOTBIS is also modifiable with NAC and it had a significant mean reduction of 12% after the first 2 cycles of NAC and approximately 17% at the end of NAC. However, no statically significant reduction was noticed in ctHHb levels. Similar finding was published by O'Sullivan *et al*. in the same work discussed before. The reduction of ctO_2Hb levels and no significant changes in ctHHb might suggest that NAC induces reduction of blood perfusion by vascular damage, and consequently, breast density reduction. It is possible that ctO_2Hb, which is more representative of arterial blood supply carrying oxygen to the breast tissue, could be more variable to meet the demands of the amount of fibroglandular tissue, resulting in a positive moderate correlation. While ctHHb, which is predominantly venous blood that carries away metabolic byproducts including deoxygenated blood after tissue consumption, may be less variable and resulting in non-correlation with the amount of fibroglandular tissue in our small sample size. While O'Sullivan *et al*. found statically reduction in ctO_2Hb levels about 90 days after start of NAC, we found a significant reduction already after 15 days. Since all patients in our study were administered taxane based regimen for the first weeks of treatment, we believe that same treatment type was responsible to minimize any variability from drug-induced changes in the breast tissue, and improved the intra and inter-patient analyses.

Regarding correlations between changes in the hemoglobin levels and tumor response to NAC, our results showed that the reduction levels of ctO_2Hb, ctTHb, ctHHb, StO_2 and water percentage were not statistically different between responders and non-responder tumors. However, after running a statistical power analyses using G*Power 3.1, a sample size of at least 40 patients would be necessary to see a statistically significant difference in the changes of ctO_2Hb levels between these two subgroups with an 80% power. Given that our study was limited by a small sample size with RCB scores available ($n = 26$), the statistical power to detect such a difference in ctO_2Hb between the two groups was only 47%. Therefore, further studies are needed to demonstrate how DOTBIS-measured parameters change within the context of response to NAC.

We also examined the relationship between baseline ctO_2Hb and age. Breast density is known to decrease with increasing patient age due to postmenopausal alteration of glandular breast tissue [32,33]. Our results presented similar association. There was a significant inverse relationship between age and ctO_2Hb measured at baseline ($p < 0.005$). As already discussed, breast tissue becomes less dense with age, therefore the correlation between the lower levels of ctO_2Hb might be related to the reduced vascular supply and perfusion occasioned by less fibroglandular tissue present in the breast of the older women.

Major limitation of our study was its dependence on the patient's mammogram availability for her inclusion in the study. The protocol at our institution does not include a post-NAC mammogram, and we were not able to have an end-point correlation between ctO_2Hb and mammographic breast density. Patient's menstrual cycles at baseline was not uniformly reported, and therefore were not accounted for analyses, which could cause variation in breast tissue composition and density assessment. In addition, we were not able to expand our analyses to correlations between MR based quantitative breast density measurement with ctO_2Hb since the majority of the women in our cohort did not had access to MR screening at pre-NAC time point. Furthermore, our study population was already diagnosed with breast cancer. Further studies in BRCA mutation carriers, a high-risk group, are needed to correlate DOTBIS-measured ctO_2Hb with breast density and how is related to cancer risk. If such a relationship can be established, it may be possible to use DOTBIS measurements to predict breast cancer risk.

Biomedical Optics EXPRESS

5. Conclusion

Optical-based image index by DOTBIS may be a novel modifiable marker of breast cancer risk that is 3D quantifiable and without exposure to ionizing radiation. Potential for its use as a predictor of breast cancer risk as well as an assessment tool to longitudinally evaluate efficacy of various chemoprevention strategies is warranted.

Funding

Breast Cancer Research Foundation; National Institutes of Health (grant 11223309).

Acknowledgments

This work was supported in part by a grant from Columbia|Biomedx - Biomedical Technology Accelerator, the Breast Cancer Research Foundation, and National Institutes of Health (grant 11223309). Furthermore, Mirella L. Altoé was supported in part by a fellowship from CNPq/LASPAU – Brazil [207913/2014-5] and Alessandro Marone was supported in part by a Personalized Medicine Fellowship of the Irving Institute for Clinical and Translational Research at Columbia University in the City of New York.

The authors thank the clinical research coordinator, Miss. Mariella Tejada, for helping with patient consenting and scheduling.

Disclosures

The authors declare that there are no conflicts of interest related to this article.

References

1. R. L. Siegel, K. D. Miller, and A. Jemal, "Cancer statistics, 2019," CA Cancer J. Clin. **69**(1), 7–34 (2019).
2. C. M. Vachon, C. H. van Gils, T. A. Sellers, K. Ghosh, S. Pruthi, K. R. Brandt, and V. S. Pankratz, "Mammographic density, breast cancer risk and risk prediction," Breast Cancer Res. **9**(6), 217 (2007).
3. V. A. McCormack and I. dos Santos Silva, "Breast density and parenchymal patterns as markers of breast cancer risk: a meta-analysis," Cancer Epidemiol. Biomarkers Prev. **15**(6), 1159–1169 (2006).
4. N. F. Boyd, H. Guo, L. J. Martin, L. Sun, J. Stone, E. Fishell, R. A. Jong, G. Hislop, A. Chiarelli, S. Minkin, and M. J. Yaffe, "Mammographic Density and the Risk and Detection of Breast Cancer," N. Engl. J. Med. **356**(3), 227–236 (2007).
5. N. F. Boyd, J. W. Byng, R. A. Jong, E. K. Fishell, L. E. Little, A. B. Miller, G. A. Lockwood, D. L. Tritchler, and M. J. Yaffe, "Quantitative classification of mammographic densities and breast cancer risk: results from the Canadian National Breast Screening Study," J. Natl. Cancer Inst. **87**(9), 670–675 (1995).
6. I. Kato, C. Beinart, A. Bleich, S. Su, M. Kim, and P. G. Toniolo, "A nested case-control study of mammographic patterns, breast volume, and breast cancer (New York City, NY, United States)," Cancer Causes Control **6**(5), 431–438 (1995).
7. J. Wei, H.-P. Chan, M. A. Helvie, M. A. Roubidoux, B. Sahiner, L. M. Hadjiiski, C. Zhou, S. Paquerault, T. Chenevert, and M. M. Goodsitt, "Correlation between mammographic density and volumetric fibroglandular tissue estimated on breast MR images," Med. Phys. **31**(4), 933–942 (2004).
8. C. Klifa, J. Carballido-Gamio, L. Wilmes, A. Laprie, J. Shepherd, J. Gibbs, B. Fan, S. Noworolski, and N. Hylton, "Magnetic resonance imaging for secondary assessment of breast density in a high-risk cohort," Magn. Reson. Imaging **28**(1), 8–15 (2010).
9. N. A. Lee, H. Rusinek, J. Weinreb, R. Chandra, H. Toth, C. Singer, and G. Newstead, "Fatty and fibroglandular tissue volumes in the breasts of women 20-83 years old: comparison of X-ray mammography and computer-assisted MR imaging," AJR Am. J. Roentgenol. **168**(2), 501–506 (1997).
10. D. B. Kopans, "Basic physics and doubts about relationship between mammographically determined tissue density and breast cancer risk," Radiology **246**(2), 348–353 (2008).
11. P. Taroni, G. Quarto, A. Pifferi, F. Abbate, N. Balestreri, S. Menna, E. Cassano, and R. Cubeddu, "Breast tissue composition and its dependence on demographic risk factors for breast cancer: non-invasive assessment by time domain diffuse optical spectroscopy," PLoS One **10**(6), e0128941 (2015).
12. B. W. Pogue, S. Jiang, H. Dehghani, C. Kogel, S. Soho, S. Srinivasan, X. Song, T. D. Tosteson, S. P. Poplack, and K. D. Paulsen, "Characterization of hemoglobin, water, and NIR scattering in breast tissue: analysis of intersubject variability and menstrual cycle changes," J. Biomed. Opt. **9**(3), 541–552 (2004).
13. P. Taroni, A. Pifferi, G. Quarto, L. Spinelli, A. Torricelli, F. Abbate, A. Villa, N. Balestreri, S. Menna, E. Cassano, and R. Cubeddu, "Noninvasive assessment of breast cancer risk using time-resolved diffuse optical spectroscopy," J. Biomed. Opt. **15**(6), 060501 (2010).

Biomedical Optics EXPRESS

14. T. D. O'Sullivan, A. Leproux, J.-H. Chen, S. Bahri, A. Matlock, D. Roblyer, C. E. McLaren, W.-P. Chen, A. E. Cerussi, M.-Y. Su, and B. J. Tromberg, "Optical imaging correlates with magnetic resonance imaging breast density and reveals composition changes during neoadjuvant chemotherapy," Breast Cancer Res. **15**(1), R14 (2013).
15. P. E. Freer, "Mammographic Breast Density: Impact on Breast Cancer Risk and Implications for Screening," Radiographics **35**(2), 302–315 (2015).
16. M. L. Flexman, M. A. Khalil, R. Al Abdi, H. K. Kim, C. J. Fong, E. Desperito, D. L. Hershman, R. L. Barbour, and A. H. Hielscher, "Digital optical tomography system for dynamic breast imaging," J. Biomed. Opt. **16**(7), 076014 (2011).
17. H. K. Kim, M. Flexman, D. J. Yamashiro, J. J. Kandel, and A. H. Hielscher, "PDE-constrained multispectral imaging of tissue chromophores with the equation of radiative transfer," Biomed. Opt. Express **1**(3), 812–824 (2010).
18. B. Brooksby, B. W. Pogue, S. Jiang, H. Dehghani, S. Srinivasan, C. Kogel, T. D. Tosteson, J. Weaver, S. P. Poplack, and K. D. Paulsen, "Imaging breast adipose and fibroglandular tissue molecular signatures by using hybrid MRI-guided near-infrared spectral tomography," Proc. Natl. Acad. Sci. U.S.A. **103**(23), 8828–8833 (2006).
19. D. Grosenick, H. Rinneberg, R. Cubeddu, and P. Taroni, "Review of optical breast imaging and spectroscopy," J. Biomed. Opt. **21**(9), 091311 (2016).
20. M. K. Simick, R. Jong, B. Wilson, and L. Lilge, "Non-ionizing near-infrared radiation transillumination spectroscopy for breast tissue density and assessment of breast cancer risk," J. Biomed. Opt. **9**(4), 794–803 (2004).
21. K. M. Blackmore, J. A. Knight, J. Walter, and L. Lilge, "The Association between Breast Tissue Optical Content and Mammographic Density in Pre- and Post-Menopausal Women," PLoS One **10**(1), e0115851 (2015).
22. J. Ruiz, F. Nouizi, J. Cho, J. Zheng, Y. Li, J.-H. Chen, M.-Y. Su, and G. Gulsen, "Breast density quantification using structured-light-based diffuse optical tomography simulations," Appl. Opt. **56**(25), 7146–7157 (2017).
23. Q. Fang, J. Selb, S. A. Carp, G. Boverman, E. L. Miller, D. H. Brooks, R. H. Moore, D. B. Kopans, and D. A. Boas, "Combined Optical and X-ray Tomosynthesis Breast Imaging," Radiology **258**(1), 89–97 (2011).
24. P. Taroni, A. Pifferi, G. Quarto, L. Spinelli, A. Torricelli, F. Abbate, A. Villa, N. Balestreri, S. Menna, E. Cassano, and R. Cubeddu, "Noninvasive assessment of breast cancer risk using time-resolved diffuse optical spectroscopy," J. Biomed. Opt. **15**(6), 060501 (2010).
25. B. T. Nicholson, A. P. LoRusso, M. Smolkin, V. E. Bovbjerg, G. R. Petroni, and J. A. Harvey, "Accuracy of assigned BI-RADS breast density category definitions," Acad. Radiol. **13**(9), 1143–1149 (2006).
26. J.-H. Chen, K. Nie, S. Bahri, C.-C. Hsu, F.-T. Hsu, H.-N. Shih, M. Lin, O. Nalcioglu, and M.-Y. Su, "Decrease in breast density in the contralateral normal breast of patients receiving neoadjuvant chemotherapy: MR imaging evaluation," Radiology **255**(1), 44–52 (2010).
27. J.-H. Chen, W.-F. Pan, J. Kao, J. Lu, L.-K. Chen, C.-C. Kuo, C.-K. Chang, W.-P. Chen, C. E. McLaren, S. Bahri, R. S. Mehta, and M.-Y. Su, "Effect of taxane-based neoadjuvant chemotherapy on fibroglandular tissue volume and percent breast density in the contralateral normal breast evaluated by 3T MR," NMR Biomed. **26**(12), 1705–1713 (2013).
28. J. A. Knight, K. M. Blackmore, J. Fan, K. E. Malone, E. M. John, C. F. Lynch, C. M. Vachon, L. Bernstein, J. D. Brooks, A. S. Reiner, X. Liang, M. Woods, and J. L. Bernstein; WECARE Study Collaborative Group, "The association of mammographic density with risk of contralateral breast cancer and change in density with treatment in the WECARE study," Breast Cancer Res. **20**(1), 23 (2018).
29. M. E. Sandberg, J. Li, P. Hall, M. Hartman, I. dos-Santos-Silva, K. Humphreys, and K. Czene, "Change of mammographic density predicts the risk of contralateral breast cancer--a case-control study," Breast Cancer Res. **15**(4), R57 (2013).
30. J. J. Noh, G. Maskarinec, I. Pagano, L. W.-K. Cheung, and F. Z. Stanczyk, "Mammographic densities and circulating hormones: a cross-sectional study in premenopausal women," Breast **15**(1), 20–28 (2006).
31. Y. Bremnes, G. Ursin, N. Bjurstam, S. Rinaldi, R. Kaaks, and I. T. Gram, "Endogenous sex hormones, prolactin and mammographic density in postmenopausal Norwegian women," Int. J. Cancer **121**(11), 2506–2511 (2007).
32. C. M. Checka, J. E. Chun, F. R. Schnabel, J. Lee, and H. Toth, "The Relationship of Mammographic Density and Age: Implications for Breast Cancer Screening," AJR Am. J. Roentgenol. **198**(3), W292 (2012).
33. L. E. Kelemen, V. S. Pankratz, T. A. Sellers, K. R. Brandt, A. Wang, C. Janney, Z. S. Fredericksen, J. R. Cerhan, and C. M. Vachon, "Age-specific trends in mammographic density: the Minnesota Breast Cancer Family Study," Am. J. Epidemiol. **167**(9), 1027–1036 (2008).